Tinospora Cordifolia Bioactive Compounds as a Novel Sterol 14a- Demethylase (Cyp51) Inhibitor: an Insilico Study

Kolawole T. Mesileya

mesileyakolawole2018@gmail.com

Afe Babalola University

precious onyeka

Afe Babalola University

Iyidola M. Adaramola

Afe Babalola University

Quareebat O. Igbalaye

Afe Babalola University

Damilola S. Bodun

Adekunle Ajasin University

Wisdom K. Alao

Afe Babalola University

Salim Y. Jibril

Afe Babalola University

Mustapha S. Mohammed

Afe Babalola University

Adedayo S. Bowaje

Afe Babalola University

Adebisi M. Adeleye

Afe Babalola University

olaposi omotuyi

Afe Babalola University

Research Article

Keywords: Tinospora cordifolia, Chagas disease, Computational models, Phyto-compounds, In-silico, Sterol 14-α-demethylase

Posted Date: December 23rd, 2024

DOI: https://doi.org/10.21203/rs.3.rs-5167713/v1

Additional Declarations: No competing interests reported.

Version of Record: A version of this preprint was published at In Silico Pharmacology on February 13th, 2025. See the published version at https://doi.org/10.1007/s40203-025-00312-w.

Abstract

Background:

For both endemic and non-endemic areas, Trypanosoma cruzi is the cause of Chagas disease, which can be life-threatening. Oversight: The entire life cycle of T. cruzi relies on the natural production of sterol through the 14-α-demethylase metabolic pathway. Many of the medications now used to treat Chagas disease have undesirable side effects and are resistant to treatment. Using bioactive chemicals from *Tinospora cordifolia,* this study attempted to anticipate the inhibitor(s) of sterol 14a-demethylase (cyp51). Utilizing the glide model, a library including one hundred twenty-two (122) compounds from *Tinospora cordifolia*was screened against sterol 14-α-demethylase (cyp51). The e-pharmacophore, pharmacokinetics profile and generalized born surface area (mm-gbsa) in molecular mechanics were performed utilizing four (4) leads and the maestro-schrodinger suite (2022).

Results:

The results indicate that the top four compounds outperform the standard drug (benznidazole). In binding affinity to 14-α-demethylase, as evidenced by docking scores ranging from -11.397 kcal/mol to -9.539 kcal/mol. Furthermore, the top compounds did not appear to be cytotoxic by ADMET projections. The hit compounds' density functional theory results showed that their Ehomo values ranged from -5.59 eV to -5.80 eV, indicating that the hit molecules are electron donors.

Conclusions:

This study identifies potential *Tinospora cordifolia* inhibitors with higher binding affinities and provides a detailed description of their interaction with the target protein. Although the results are favorable, further in vivo and in vitro studies are required to confirm these compounds' potential as anti-Chagas agents.

1. BACKGROUND

The protozoan known as American trypanosomiasis, or Chagas disease (CD), is one of the neglected tropical diseases (NTDs) that is spread by kissing bugs (Omoboyowa, 2022). According to Lidani et al. (2019), the illness is a major public health risk in most of the nations where it is common. The World Health Organization (WHO) estimates that 6–7 million individuals worldwide suffer from CD. It is commonly contracted by humans and other mammals in rural Latin American countries through contact with the urine or dung of kissing bugs, also known as triatomine bugs (Conlan and Lal., 2015). The disease is currently common outside of Latin American nations as a result of migration from these endemic areas to Japan, the US, Canada, and Australia (Ribeiro et al., 2012). The three stages of Chagas disease—acute, indeterminate, and chronic—are fully contracted by the host whenever they come into touch with T. cruzi (Buckner, 2008).

Since most infected individuals have relatively non-specific clinical symptoms, the acute stage of Chagas disease appears soon after infection because the majority of infected people have vague clinical signs. Furthermore, the condition's diagnosis is rendered more difficult by the application of outdated and subjective approaches (Antas et al., 1999). Benznidazole and Nifurtimox were the first treatments for CD for

a long time. Because CD is seen as a neglected ailment, pharmaceutical companies are not in competition to meet manufacturing demands. It is noteworthy that the high cost of the existing and exclusive CD medications prevents individuals with CD from affording them (Pinheiro et al., 2017).

The synthesis of sterols by 14-α-demethylase is a crucial step in the life cycle of T. cruzi (Omoboyowa, 2022). In mammals, cholesterol is biosynthesized by the protease sterol 14-α-demethylase. T. cruzi's sterol production pathway is particularly intriguing for therapeutic development since the parasite is unable to use host cholesterol and is solely dependent on physiologically active sterols for growth and survival (Lepesheva et al., 2011).

Menispermaceae, the family of moonseeds, includes *T. cordifolia*, often known as Guduchi, a naturally occurring herbal shrub (Tiwari et al., 2018). About 32 species of climbing shrubs in the genus Tinospora (*Menispermaceae)* are found in tropical Africa, Madagascar, Australia, and the Pacific Islands (Udayan et al., 2009).In Ayurvedic medicine, *T. cordifolia* is classified as a "Rasayana" and is used as a tonic and vitalizer, as well as a treatment for diabetes, skin conditions, heart conditions, jaundice, rheumatoid arthritis, allergies, leprosy, urinary tract issues, and dysentery. While the stems demonstrated hepatoprotective, antipyretic, cytotoxic, antidiabetic, and immunomodulatory action, the entire plant is said to have hepatoprotective, antiulcer, and antioxidant qualities (Singh and Chaudhuri, 2017). It contains a multitude of chemical constituents, including ß-Sitosterol, cordifolioside A, B, and C, cordifoliside D and E, tinosporine (S), magnoflorine, giloinsterol (S), and palmatosides C and F. These constituents fall into various classes of bioactive compounds, including lignans, terpenoids, glycosides, aliphatic compounds, and polysaccharides (Upadhyay et al., 2010).

The possibility of phytochemicals from *Tinospora cordifolia* acting as inhibitors against T. cruzi 14-α-demethylase protease was examined using a computer-aided molecular modeling technique. This thorough method uses the pharmacophore hypothesis, quantum calculations via Density Functional Theory (DFT), MM/GBSA, molecular docking, and ADMETox screening to screen a library of phytochemicals from *Tinospora cordifolia.*

2. METHODS

2.1 Retrieval of receptors

The Protein Data Bank (PDB) (pdb: 4CKA) provided the 3D structures of T. cruzi 14-α-demethylase protease. These PDB files were processed in Maestro, where the protein preparation wizard was used to process the protein. Strict energy minimization, the insertion of absent side chains, the elimination of water and unconventional ligands, and the modification of hydrogen positions were all part of the preparation process. The Ramachandran plot was also retrieved from the preparation module and used to evaluate the quality of the protein structure.

2.2 Ramachandran plot:

The Ramachandran plot (Ramachandran et al. 1966) shows the statistical range of the likely values of Phi and Psi (dihedral angles) for the unidentified amino acid (X) found in the Ala-X-Ala tripeptide. After the

protein was produced, Fig. 1 showed the Ramachandran plot. The secondary structure of the protein T. cruzi 14-α-demethylase is described by the psi and phi predicted values, which are represented by the Ramachandran plot in Fig. 1. The secondary structure's alpha helix or beta-sheet nature is determined by the positive or negative values of the torsional values, which are based on the arrangement of the protein's amino acid sequence.

2.3 Preparation of compounds from Tinospora Cordifolia:

One hundred and twenty-two (122) reported compounds that were active compounds from *Tinospora cordifolia* were downloaded in SDF format, together with the reference molecule (benznidazole) from the literature (Sharma et al., 2022), (Saha and Ghosh, 2012), and (Singh and Chaudhuri, 2017). These compounds were "LigPrep-ed" for the OPLS_2005 force field after being added to the Schrodinger workspace. Additionally, the T. cruzi 14-α-demethylase protease Co-ligand ((1s)-1-(4-Fluorophenyl)-2-(1h-Imidazol-1-Yl)ethyl 4-Isopropylphenylcarbamate) was discovered and acquired from PubChem. After that, it was prepared in a manner akin to that of the other ligands and utilized as a reference in conjunction with the standard drug (benznidazole).

2.4 Receptor grid generation

The size and binding orientation of the active site for protein-ligand docking are determined during the receptor grid creation process. The Grid Generation Module was utilized in this investigation to calculate the receptor grid coordinates of T. cruzi 14-α-demethylase protease binding pockets, taking into account the co-crystallized ligands. For every protein target, a distinct grid box was made and placed in line with the location of the corresponding co-crystallized ligands. The receptor grid box was generated with the three-dimensional coordinates x = 0.38 Å, y = 26.32 Å, and z = 460.09 Å.

2.5 Molecular docking:

Docking was done on Maestro 13.4 (Schrödinger 2022) using the Glide tool (Friesner et al., 2004). Using the three hierarchical docking filtering methodologies, benznidazole the reference drug, co-crystallized ligand and one hundred and twenty-two (122) compounds from *Tinospora cordifolia* were virtually screened. The large number of ligands was quickly screened using high-throughput virtual screening (HTVS) docking precision, which has considerably more limited conformational sampling than existing precision filters. Thus, using HTVS docking, the 122 compounds were screened against T. cruzi 14-α-demethylase protease. The standard precision (SP) filtering technology was utilized to conduct additional screening on the top twenty hit compounds. Using the extra precision (XP) scoring algorithm, four (4) hits that had docking affinity greater than the reference medication (benznidazole) were screened further, respectively.

2.5 Hits virtually screening with E-pharmacophore model:

An energy-optimized pharmacophore model was developed for the crystal structure of T. cruzi 14-α-demethylase protease (4CKA) using the co-crystallized ligand (1s)-1-(4-Fluorophenyl)-2-(1h-Imidazol-1-Yl) ethyl 4-Isopropylphenylcarbamate. The protein-ligand option of the phase-develop pharmacophore tool of the Schrodinger suite (2022) was used for developing the model (Omoboyowa, 2022). The four (4) hit compounds from the docking scores were used for the virtual screening based on e-pharmacophore. The pharmacophore-based analysis was performed with a phase module to produce a subset of molecules with

chemical features for binding to 4CKA in accordance with the created model. The hit compounds were prepared utilizing macro model minimization. The finest hits were justified based on the fitness scores.

2.6 ADME/Tox screening:

The pharmacokinetic profile, drug-likeness, and toxicity of the hit compounds were evaluated along with the absorption, distribution, metabolism, excretion, and toxicity (ADMET) properties using the AdmetSar web server, swissadme web server, and the QikProp module within the Schrodinger's Maestro interface.

2.7 MM/GBSA:

The Molecular Mechanics/Generalized Born Surface Area (MM/GBSA) continuum solvent model was used for calculating the docked protein-ligand complex binding free energy. Prime's rotamer search techniques were integrated with the OPLS3 force field and the VSGB solvent model.

2.8 Density Functional Theory (DFT):

Density functional theory (DFT) and quantum chemistry studies were used to assess the molecular properties of an Andrographis Paniculate molecule in order to predict the biological activities of the compounds that ranked highest. After calculating the conformer distribution using the computational chemistry application Spartan 10 to perform DFT analysis in a vacuum, the most stable conformer was selected. This research yielded the thermodynamic parameters EHOMO and ELUMO. These values were then used to create further features and the global reactivity descriptors. For example, the energy band gap was computed using the difference between ELUMO and EHOMO.

(Eg) = ELUMO-EHOMO (1)

While Koopman's theory connects the Ionization energy (I) and Electron Affinity (A) to EHOMO and ELUMO (Koopmans, 1993).

I = -EHOMO (2)

A = -ELUMO (3)

$\chi = 1 + A / 2$ (4)

$\eta = 1-A / 2$ (5)

$\delta = 1 / n$ (6)

3. RESULTS

3.1 Docking/MMGBSA:

The docking scores and MM/GBSA screening outcomes for the hit compounds are represented graphically in Fig. 2 and Table 1, respectively, with their chemical structures depicted in Fig. 5. To assess the potential inhibitory effects of the chosen *Tinospora Cordifolia* ligands, the target protein's T. cruzi 14-α-demethylase

protease binding pocket was docked with enhanced precision (XP). Along with looking at the structural interactions of the top compounds, the important amino-acid interactions at the T. cruzi 14-α-demethylase protease binding site were discovered.

Table 1
The binding affinity (kcal/mol) and MMGBSA of the top-ranked *Tinospora Cordifolia* phytochemical constituents and standard drug against the T. cruzi 14-α-demethylase protease target.

s/n	Compound name	PubChem Cid	docking score(kcal/mol)	mmgbsa (Δg bind)
1	Epicatechin	107905	-11.397	-23.88
2	N-trans-caffeoyltyramine	9994897	-10.918	-42.15
3	Co-crystallized Ligand	76871876	-10.653	-24.92
4	N-trans-Feruloyl tyramine	5280537	-10.254	-39.3
5	Paprazine	5372945	-9.539	-45.53
6	Benznidazole (standard drug)	31593	-5.892	-38.62

A range of docking scores for each of the four ligands are shown in Table 1 and Fig. 2. Epicatechin had a docking score of 11.397 kcal/mol, while N-trans-caffeoyl tyramine had a value of 10.918 kcal/mol. Additionally, the docking scores for paprazine and N-trans-Feruloyl tyramine are − 9.539 kcal/mol and − 10.254 kcal/mol, respectively. in contrast to the co-crystallized ligand, which had a docking score of -10.653 kcal/mol, and the standard drug (benznidazole), which had a docking value of -5.892 kcal/mol. Epicatechin, on the other hand, has a noticeably higher binding affinity.

The robust MM/GBSA tool in Schrodinger's suite was utilized to further validate the docking studies of the hit compounds by calculating the binding free energy of the docked protein-ligand complexes. MM/GBSA provides a precise determination of the binding energy and structural stability of protein-ligand complexes (Omoboyowa et al., 2022). Several studies have also confirmed the accuracy of MM-GBSA as a post-docking technique for identifying the binding location of docked complexes (Tripathi et al., 2013). Table 1 and Fig. 2 displays the binding energies of the compounds. With higher binding energy (-45.53) than both the co-crystallized ligand (-24.92) and the standard drug (benznidazole) (-38.62), Paprazine demonstrated a better interaction with the target proteins.

To evaluate the inhibitory capacity of the selected *Tinospora cordifolia* ligands, the T. cruzi 14-α-demethylase protease (4CKA) binding pocket was docked using extra precision (XP). Moreover, we examined the critical amino-acid interactions in the T. cruzi 14-α-demethylase protease binding area and the structural correlations among the leading compounds, the standard molecule, and the co-crystallized ligand.

Figure 3 displays the two-dimensional molecule interaction, whereas Fig. 4 demonstrates the three-dimensional molecular interaction. Table 2 and Fig. 3 demonstrated that two hydrogen bonds were formed by Epicatechin with ALA291 and MET358 with pi-pi stacking with TYR103 and hem1480. N-trans-caffeoyltyramine formed two hydrogen bonds with MET358 and TYR116 and pi-pi stacking with TYR103, while the co-crystallized ligand formed one hydrogen bond with TYR116 and pi-pi stacking with HEM1480

and TYR103. N-trans-feruloyl tyramine formed one hydrogen bond with the amino acid TYR116 and no pi-pi stacking. Paprazine formed two hydrogen bonds with amino acids MET358 and TYR116 and pi-pi stacking with TRY103. Additionally, the standard drug Benznidazole formed two hydrogen bonds with the amino acids TYR103 and TYR116 and pi-pi stacking with TYR103.

Table 2
Molecular contact profiling of the top *Tinospora Cordifolia* phytochemicals, the standard drug and Co-crystallized Ligand.

COMPOUND NAME	H-BOND INTERACTION	HYDROPHOBIC AMINO ACID	OTHER INTERACTION
Epicatechin	ALA291, MET358,	ALA291, PHE290, ALA388, ALA287, LEU130, MET123, PHE110, LEU127, TRY103, TYR116, VAL213, ALA115, MET106, VAL359, MET358, LEU356, MET460, VAL461	PI-PI STACKING:TYR103, HEM1480
N-trans-caffeoyltyramine	MET358, TYR116	ALA291, PHE290, ALA288, ALA287, MET284, LEU130, LEU127, PHE110, ALA115, TYR116, MET123, TYR103, MET106, MET360, VAL359, MET358, LEU356.	PI-PI STACKING:TYR103
Co-crystallized Ligand	TYR116	LEU356, ALA391, PHE290, PHE110, ALA288, ALA287, TYR116, ALA115, VAL114, MET123, MET284, LEU127, ILE423, LEU130, MET106, ILE105, LEU208, MET460, TYR103	PI-PI STACKING:HEM1480, TYR103
N-trans-Feruloyl tyramine	TYR116	MET123, MET284, ALA287, ALA288, PHE110, PHE290, ALA291, MET360, VAL359, MET358, VAL213, LEU356, TYR103, LEU208, MET460, ILE105, LEU130, LEU127, TYR116, MET106, ALA115	PI-PI STACKING: NONE
Paprazine	MET358, TYR116	ALA291, PHE290, ALA288, ALA287, MET284, LEU130, LEU127, PHE110, ALA115, TYR116, MET123, TYR103, MET106, VAL359, MET358, LEU256	PI-PI STACKING: TYR103
standard drug Benznidazole	TYR116, TYR103	LEU130, ALA291, ALA288, LEU127, ALA287, MET123, PHE110, ALA115, TYR116, TYR103, MET106, VAL359, MET358, LEU356	PI-PI STACKING: TYR103

3.2 Generation of E-pharmacophore model:

A crucial computer model for drug development without knowledge of macromolecular protein structure is the ligand-based pharmacophore method. According to Yang (2010), this theory describes a collection of steric and electrical properties that are essential for guaranteeing molecular interactions with particular biological molecules and for activating or suppressing the signaling pathways of these proteins. Here, the co-crystallized protein complex served as the basis for the development of the e-pharmacophore model. Four partitioning features were used to identify the hypothesis model.

The derived hypothesis is displayed in Fig. 7 along with the target's co-crystallized ligand. One hydrogen bond donor, three aromatic rings, and two hydrophobic contacts are present in the model with the highest fitness score. Figure 6 illustrates the specific pharmacophore features, where H5 and H6 are hydrophobic regions (green), R8, R9, and R10 are aromatic rings (orange), and D4 is a hydrogen bond donor (blue). Table 3 displays the fitness ratings of the four (4) hit compounds and co-crystallized ligands that were selected based on these attributes throughout the screening process for *Tinospora cordifolia.* With a score of 1.128, paprazine has the highest rating, followed by N-trans-Feruloyl tyramine (1.051). Despite this, the fitness ratings of all the hit compounds were lower than the co-crystallized ligands, which was 2.32.

Table 3
Fitness scores of hit compounds from the E-pharmacophore model

s/n	Compound name	PubChem Cid	Fitness scores
1	Epicatechin	107905	0.961
2	N-trans-caffeoyltyramine	9994897	0.967
3	Co-crystallized Ligand	76871876	2.32
4	N-trans-Feruloyl tyramine	5280537	1.051
5	Paprazine	5372945	1.128

Table 4
In-silico drug-likeness, oral bio-availability, pharmacokinetic properties, Toxicity profile, and Cytochrome P450 metabolizing enzymes inhibitory potentials of selected *Tinospora Cordifolia* phytochemical constituent, Co-crystallized ligand and standard drug

Compound name	Epicatechin	N-trans-caffeoyltyramine	Co-crystallized Ligand	N-trans-Feruloyl tyramine	Paprazine	standard drug
MW g/mol	442.37	299.32	367.42	313.35	283.32	260.25
BBB permeant	NO	NO	YES	NO	YES	NO
GI absorption	LOW	HIGH	HIGH	HIGH	HIGH	HIGH
PGP Substrate	NO	NO	NO	NO	NO	NO
CYP1A2 inhibitor	NO	NO	YES	NO	NO	NO
CYP2C19 inhibitor	NO	NO	YES	NO	NO	NO
CYP2C9 inhibitor	NO	YES	YES	NO	NO	NO
CYP2D6 inhibitor	NO	YES	YES	YES	YES	NO
CYP3A4 inhibitor	NO	YES	YES	YES	YES	NO
Bioavailability Score	0.55	0.55	0.55	0.55	0.55	0.55
Hepatotoxicity	active	inactive	active	Inactive	Inactive	active
Carcinogenicity	inactive	inactive	inactive	inactive	inactive	Inactive
Nephrotoxicity	inactive	inactive	Inactive	inactive	Inactive	inactive
Rule of five (5)	1	0	1	0	0	0

3.3 Pharmacokinetic screening:

An important pharmacokinetic screening test is the measurement of blood-brain barrier (BBB) permeability, which has two functions: it determines the degree to which potential medications are bioavailable to the central nervous system (CNS) and keeps harmful compounds out of the brain. Notwithstanding the possibility of accuracy issues with computer-aided assessment of BBB permeability, the discovery of novel therapeutic candidates has proven to be a time- and money-saving approach.

Drug-drug interactions (DDIs) can result from drugs that inhibit specific CYP isoforms, such as CYP1A2, CYP2C19, CYP2C9, CYP2D6, and CYP3A4, which are involved in the metabolism of many pharmaceuticals. The top compound in Table 4 and Fig. 8, epicatechin, did not show any inhibitory effect on various CYP isoforms, indicating that it is unlikely that these chemicals will have an impact on other medicinal drugs' metabolism.

Drug-drug interactions (DDI) may occur as a result of the similarities between CYP34A substrate medications and P-glycoprotein substrate pharmaceuticals. P-glycoprotein substrates are excreted in bile and urine, which reduces their bioavailability and raises P-gp clearance (Finch and Pillans, 2014). The in silico research conducted for this study indicates that every molecule examined in Table 4 is a P-gp substrate.

In pharmacology, "bioavailability" refers to the extent and pace of absorption and transformation of a bioactive molecule into a condition that can be utilized (Kim et al., 2014). Drug discovery is frequently hampered by limited oral bioavailability, which can lead to molecules exhibiting excellent performance in vitro and in vivo studies but failing in clinical trials as a result (Erhirhie et al., 2018). A bioavailability score above 0.5 indicates high oral bioavailability and a score below 0.5 indicates low oral bioavailability, according to research by Rath et al. (2021). With a bioavailability score of 0.55 for each chemical in Table 4, excellent oral bioavailability is indicated. (-) Epicatechin and the co-crystallized ligand are active in hepatotoxicity, although N-trans-feruloyl and N-trans-caffeoyl tyramine are not. On the other hand, the standard drug has hepatotoxicity activity, indicating possible liver toxicity issues. There is no possibility that any of the compounds, including standard drugs, might cause cancer because they are all inert in terms of carcinogenicity. Aside from epicatechin (-), none of the compounds exhibit any nephrotoxicity, indicating a low probability of kidney toxicity linked to these compounds.

TABLE 5: STRUCTURES OF THE LIGANDS IN OPTIMIZED, HOMO AND LUMO FORM.

COMPOUND	OPTIMIZED	E HOMO	E LUMO
Epicatechin	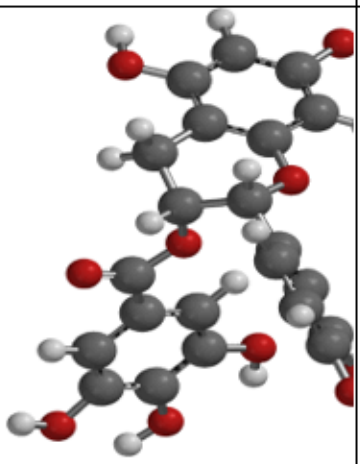	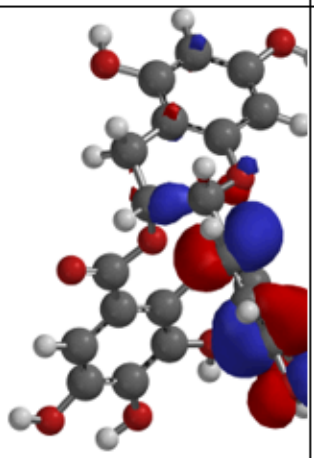	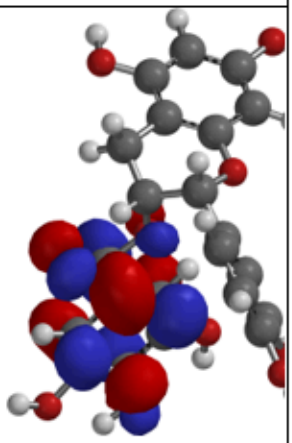
N-trans-caffeoyltyramine	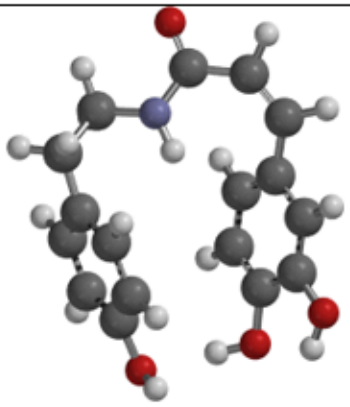	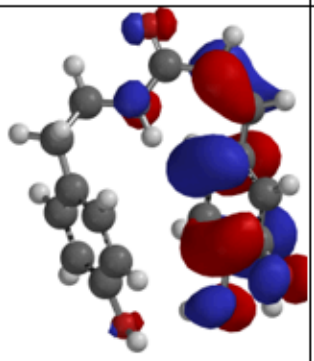	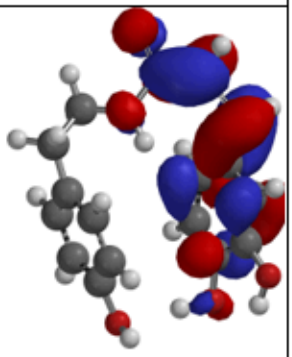
N-trans-Feruloyl tyramine	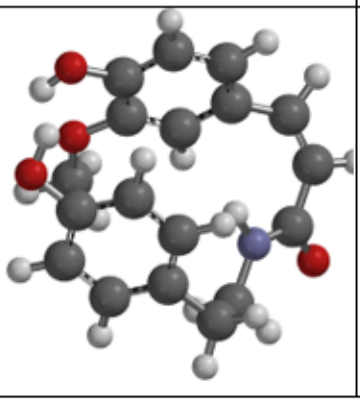	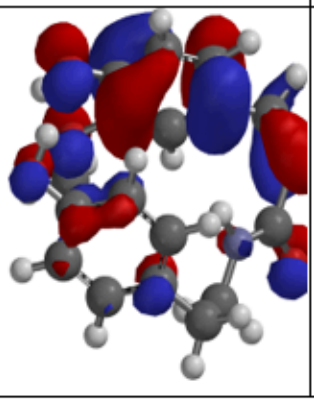	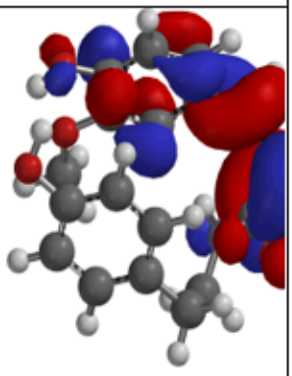

Paprazine	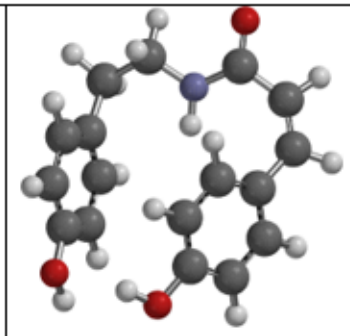	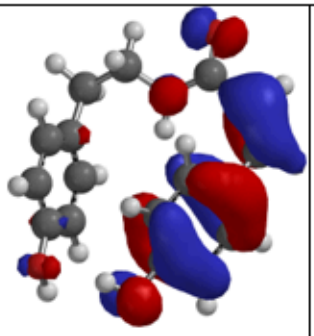	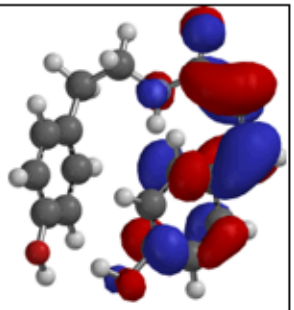
standard drug	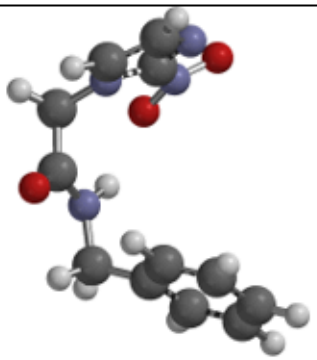	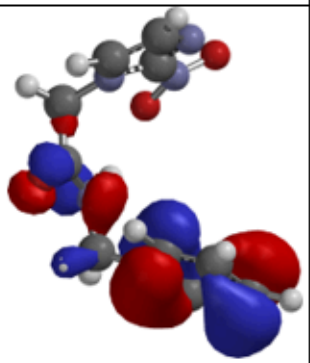	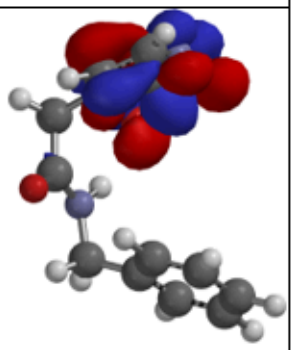

Table 6
THE CALCULATED THERMODYNAMIC QUANTITIES (ENTHALPY AND FREE ENERGY) VIA DFT

COMPOUND	E_{HOMO} (eV)	E_{LUMO} (eV)	E_g (eV)	I((eV)	A(eV)	η (eV)	δ (eV^{-1})	χ (eV)	⊠(eV)
Epicatechin	-5.59	-1.04	4.55	5.59	1.04	2.275	0.43956	3.315	2.415214
N-trans-caffeoyltyramine	-5.74	-1.16	4.58	5.74	1.16	2.29	0.436681	3.45	2.598799
N-trans-Feruloyl tyramine	-5.77	-2.27	3.5	5.77	2.27	1.75	0.571429	4.02	4.617257
Paprazine	-5.80	-1.14	4.66	5.8	1.14	2.33	0.429185	3.47	2.583884
standard drug	-6.69	-2.76	3.93	6.69	2.76	1.965	0.508906	4.725	5.680821

3.4 Density Functional Theory:

Frontier Molecular Orbitals (FMOs)

The energies of the Frontier Molecular Orbitals (FMOs) reveal crucial details about a substance's reactivity. While the HOMO energy explicitly shows a molecule's capacity to donate electrons, the LUMO energy predicts how a molecule can accept electrons. These FMOs and the HOMO-LUMO orbitals are crucial for figuring out the optical and electrical characteristics of molecules.

A greater HOMO energy indicates that a molecule is more likely to provide electrons, while a lower LUMO energy indicates a higher probability of accepting electrons, increasing the reactivity of the molecule

(Olugbogi et al., 2023). The compounds under investigation have electron-accepting capacity, as evidenced by their ELUMO values, which span from − 1.04 eV to -2.76 eV. Among hit compounds, N-trans-Feruloyl tyramine is unique in that it exhibits a greater electron-accepting activity.

The band gap energy, which lies between the EHOMO and ELUMO, has a big impact on a molecule's thermochemical reactivity. Band gap energy levels provide information on the chemical stability and reactivity of a molecule. In contrast to a molecule with a narrower band gap, which has greater reactivity and less stability, one with a larger band gap is tougher, more stable, and has less reactivity.

Tables 5 and 6 display the optimized HOMO and LUMO structures of the compounds, together with a list of their electronic affinities ranging from 1.04 eV to 2.76 eV. Table 6 also provides the calculated thermodynamic parameters (enthalpy and free energy) of the expected inhibitors as determined by DFT.

The reactivity of the compounds was verified through the assessment of their chemical hardness, softness, electronegativity, and chemical potential using the global reactivity descriptor (GRD).

Chemical hardness (η) is the capacity of a molecule to withstand the deformation caused by an electron cloud. Hard molecules are less polarizable and have a wider energy band gap than soft molecules, which have a lower band gap. Among the compounds under investigation, Paprazine had the highest hardness value (2.33 eV), while N-trans-Feruloyl tyramine had the lowest (1.75 eV). Out of all the compounds examined, all of which fell within a tight range, the standard drug (benzodazole) had the highest electronegativity, recording 4.725 eV. Electronegativity (χ) is the capacity of a molecule to absorb electrons during a chemical reaction. Table 5 displays the optimized HOMO and LUMO structures of the compounds. The electronic affinities of the predicted inhibitors range from 0.04 to -2.76 eV. Table 6 shows the calculated thermodynamic parameters (enthalpy and free energy) of the predicted inhibitors using DFT.

4. DISCUSSION

This study explored the inhibitory potential of bioactive compounds from *Tinospora cordifolia* against sterol 14-α-demethylase (CYP51), a key enzyme in the life cycle of Trypanosoma cruzi, the pathogen responsible for Chagas disease. Among the compounds, Epicatechin exhibited the highest docking score (-11.397 kcal/mol), surpassing the standard treatment drug Benznidazole (-5.892 kcal/mol) and the co-crystallized ligand (-10.653 kcal/mol). This suggests that Epicatechin may have a stronger binding affinity, positioning it as a promising candidate for further investigation (Omoboyowa et al., 2022). Similarly, Paprazine demonstrated a notable binding energy of -45.53 kcal/mol, surpassing both the standard drug and co-crystallized ligand, indicating a robust interaction with CYP51.

Pharmacokinetic profiling supported the drug-like properties of these lead compounds. All compounds demonstrated favorable oral bioavailability, with scores of 0.55, exceeding the minimum threshold for acceptable oral absorption (Erhirhie et al., 2018). Additionally, the absence of significant carcinogenicity and nephrotoxicity in most of the lead compounds bolsters their safety profile, suggesting that natural compounds from *Tinospora cordifolia* could serve as viable alternatives to conventional treatments for parasitic diseases.

The application of Density Functional Theory (DFT) provided further insight into the electronic properties of the compounds, with favorable thermodynamic parameters such as enthalpy, free energy, and global reactivity descriptors (GRDs) like chemical hardness and electronegativity (Olugbogi et al., 2023). Paprazine, in particular, stood out due to its advantageous reactivity profile, reinforcing its potential as a strong drug candidate.

However, while these in silico results are promising, experimental validation through in vitro and in vivo studies remains essential to confirm the efficacy and safety of these compounds in biological systems. Further experimental testing is crucial to translate these computational findings into potential therapeutic applications.

4. CONCLUSIONS

One important therapeutic target for the development of drugs to treat Chagas disease is sterol-14-α-demethylase. The purpose of the study was to use computational models to predict strong sterol-14-α-demethylase antagonists from *Tinospora cordifolia* compounds that can inhibit the protein's active site. The compounds were subjected to virtual ADME screening, quantum chemistry calculations, MM/GBSA calculations, and molecular docking.

Certain compounds found in *Tinospora cordifolia*, including (-) epicatechin, N-trans-caffeoyl tyramine, N-trans-Feruloyl tyramine, and paprazine, have been identified by the study as possible therapies that can target T. cruzi 14-α-demethylase protease in the treatment of chagas disease. However, further investigation is required to evaluate and verify these findings, including the extraction of these compounds for in vitro testing to validate and fully realize the therapeutic potential of these compounds.

Abbreviations

CYP51- Sterol 14a-Demethylase.

MM-GBSA: Molecular mechanics generalized Born surface area.

PDB: Protein database.

CYP: Cytochrome.

ADMET: Absorption, Distribution, Metabolism, Excretion and Toxicity.

BBB-: Blood Brain Barrier permeability negative.

MW: Molecular Weight.

Declarations

Ethics Approval and Consent to Participate:

Not applicable.

Consent to publication:

Not applicable.

Availability of data and material:

All results, discussions, and details regarding the methods and materials used in this study are available within the submitted manuscript. This includes the 3D structures of T. cruzi 14-α-demethylase protease (PDB: 4CKA), molecular docking results, e-pharmacophore models, Density Functional Theory, and ADMET/Tox screening data. If additional information or data is required and not available within the manuscript, readers may request it from the corresponding author.

Conflict of Interests:

The authors declare that there is no conflict of interest regarding the publication of this paper.

Funding:

This research received no external funding.

Authors' Contributions:

K.T.M. conceptualized the study, wrote the original draft, and contributed to the methodology.

P.C.O. contributed to formal analysis, reviewing, and conceptualization.

I.M.A. and Q.O.I. were responsible for methodology.

D.S.B. performed visualization, validation, result analysis, and contributed to editing and reviewing the manuscript.

A.S.B. and W.K.A. contributed to editing and reviewing the manuscript.

S.Y.J. and A.M.A. contributed to reviewing.

M.S.M. performed visualization.

O.I.O. supervised the project and provided validation.

All authors have read and approved the final manuscript.

Acknowledgments:

We acknowledge the management of the research unit (MOLS & SIMS) for the provision of the needed facilities for this research work.

References

1. Omoboyowa, D. A. (2022). Exploring molecular docking with E-pharmacophore and QSAR models to predict potent inhibitors of 14-α-demethylase protease from Moringa spp. Pharmacological Research-Modern Chinese Medicine, 4, 100147. doi:10.1016/j.prmcm.2022.100147
2. Lidani, K. C. F., Andrade, F. A., Bavia, L., Damasceno, F. S., Beltrame, M. H., Messias-Reason, I. J., & Sandri, T. L. (2019). Chagas disease: from discovery to a worldwide health problem. Frontiers in public health, 7, 166. doi:10.3389/fpubh.2019.00166
3. Conlan, J., & Lal, A. (2015). Socioeconomic burden of foodborne parasites. In Foodborne parasites in the food supply web (pp. 75-98). Woodhead Publishing. doi:10.1016/B978-1-78242-332-4.00005-9
4. Ribeiro, A. L., Nunes, M. P., Teixeira, M. M., & Rocha, M. O. (2012). Diagnosis and management of Chagas disease and cardiomyopathy. Nature Reviews Cardiology, 9(10), 576-589. doi:10.1038/nrcardio.2012.109.
5. Buckner, F. S. (2008). Sterol 14-demethylase inhibitors for Trypanosoma cruzi infections. Drug targets in kinetoplastid parasites, 61-80. DOI:10.1007/978-0-387-77570-8_6
6. Antas, P. R., Medrano-Mercado, N., Torrico, F., Ugarte-Fernandez, R., GÃ³mez, F., Oliveira, R. C., ... & AraÃºjo-Jorge, T. C. (1999). Early, intermediate, and late acute stages in Chagas' disease: a study combining anti-galactose IgG, specific serodiagnosis, and polymerase chain reaction analysis. The American journal of tropical medicine and hygiene, 61(2), 308-314. DOI:10.4269/ajtmh.1999.61.308
7. Pinheiro, E., Brum-Soares, L., Reis, R., & Cubides, J. C. (2017). Chagas disease: review of needs, neglect, and obstacles to treatment access in Latin America. Revista da sociedade brasileira de medicina tropical, 50, 296-300. doi:10.1590/0037-8682-0433-2016
8. Lepesheva, G. I., Villalta, F., & Waterman, M. R. (2011). Targeting Trypanosoma cruzi sterol 14α-demethylase (CYP51). Advances in parasitology, 75, 65-87. doi:10.1016/B978-0-12-385863-4.00004-6
9. Tiwari, P., Nayak, P., Prusty, S. K., & Sahu, P. K. (2018). Phytochemistry and pharmacology of Tinospora cordifolia: A review. *Systematic Reviews in Pharmacy*, *9*(1), 70-78. doi:10.5530/srp.2018.1.14
10. Udayan, P. S., Pradeep, A. K., & Balachandran, I. (2009). A new species of Tinospora (Menispermaceae) from South India. *Edinburgh Journal of Botany*, *66*(1), 77-80. doi:10.1017/S0960428609005204
11. Singh, D., & Chaudhuri, P. K. (2017). Chemistry and pharmacology of Tinospora cordifolia. *Natural product communications*, *12*(2), 1934578X1701200240. doi:10.1177/1934578X1701200240
12. Upadhyay, A. K., Kumar, K., Kumar, A., & Mishra, H. S. (2010). Tinospora cordifolia (Willd.) Hook. f. and Thoms.(Guduchi)–validation of the Ayurvedic pharmacology through experimental and clinical studies. *International journal of Ayurveda research*, *1*(2), 112. doi:10.4103/0974-7788.64405
13. Ramachandran, G. N., Venkatachalam, C. M., & Krimm, S. (1966). Stereochemical criteria for polypeptide and protein chain conformations: III. Helical and hydrogen-bonded polypeptide chains. *Biophysical journal*, *6*(6), 849-872. DOI:10.1016/S0006-3495(66)86699-7
14. Sharma, P., Dwivedee, B. P., Bisht, D., Dash, A. K., & Kumar, D. (2019). The chemical constituents and diverse pharmacological importance of Tinospora cordifolia. *Heliyon*, *5*(9). doi:10.1016/j.heliyon.2019.e02437
15. Saha, S., & Ghosh, S. (2012). Tinospora cordifolia: One plant, many roles. *Ancient science of life*, *31*(4), 151. DOI: 10.4103/0257-7941.107344

16. Singh, D., & Chaudhuri, P. K. (2017). Chemistry and pharmacology of Tinospora cordifolia. *Natural product communications*, *12*(2), 1934578X1701200240. doi:10.1177/1934578X1701200240 https://pubchem.ncbi.nlm.nih.gov
17. Friesner, R. A., Banks, J. L., Murphy, R. B., Halgren, T. A., Klicic, J. J., Mainz, D. T., ... & Shenkin, P. S. (2004). Glide: a new approach for rapid, accurate docking and scoring. 1. Method and assessment of docking accuracy. *Journal of medicinal chemistry*, *47*(7), 1739-1749. doi:10.1021/jm0306430.
18. Omoboyowa, D. A. (2022). Exploring molecular docking with E-pharmacophore and QSAR models to predict potent inhibitors of 14-α-demethylase protease from Moringa spp. *Pharmacological Research-Modern Chinese Medicine*, *4*, 100147. doi:10.1016/j.prmcm.2022.100147
19. SwissADME (http://www.swissadme.ch)
20. AdmetSar http://lmmd.ecust.edu.cn/admetsar2/
21. Koopmans, T. (1933). Ordering of wave functions and eigenenergies to the individual electrons of an atom. *Physica*, *1*, 104-113. DOI:10.1016/S0031-8914(34)90011-2
22. Omoboyowa, D. A., Iqbal, M. N., Balogun, T. A., Bodun, D. S., Fatoki, J. O., & Oyeneyin, O. E. (2022). Inhibitory potential of phytochemicals from Chromolaena odorata L. against apoptosis signal-regulatory kinase 1: A computational model against colorectal cancer. *Computational Toxicology*, *23*, 100235. DOI:10.1016/j.comtox.2022.100235
23. Tripathi, S. K., Muttineni, R., & Singh, S. K. (2013). Extra precision docking, free energy calculation, and molecular dynamics simulation studies of CDK2 inhibitors. *Journal of theoretical biology*, *334*, 87-100. DOI:10.1016/j.jtbi.2013.05.014
24. Yang, S. Y. (2010). Pharmacophore modeling and applications in drug discovery: challenges and recent advances. *Drug discovery today*, *15*(11-12), 444-450. doi.org/10.1016/j.drudis.2010.03.013
25. Finch, A., & Pillans, P. (2014). P-glycoprotein and its role in drug-drug interactions. *Aust Prescr*, *37*(4), 137-139. DOI:10.18773/austprescr.2014.050
26. Kim, M. T., Sedykh, A., Chakravarti, S. K., Saiakhov, R. D., & Zhu, H. (2014). Critical evaluation of human oral bioavailability for pharmaceutical drugs by using various cheminformatics approaches. *Pharmaceutical research*, *31*, 1002-1014. DOI:10.1007/s11095-013-1222-1
27. Erhirhie, E. O., Ihekwereme, C. P., & Ilodigwe, E. E. (2018). Advances in acute toxicity testing: strengths, weaknesses and regulatory acceptance. *Interdisciplinary toxicology*, *11*(1), 5-12. DOI: 10.2478/intox-2018-0001
28. Rath, B., Qais, F. A., Patro, R., Mohapatra, S., & Sharma, T. (2021). Design, synthesis, and molecular modeling studies of novel mesalamine-linked coumarin for treatment of inflammatory bowel disease. *Bioorganic & Medicinal Chemistry Letters*, *41*, 128029. DOI:10.1016/j.bmcl.2021.128029
29. Olugbogi , E. A. O. (2023, April 1). *COMPUTER-BASED SCREENING OF THE ANTICANCER PROPERTY OF SELECTED PANAX GINSENG PHYTO-LIGANDS*. Ijpsr. Retrieved April 5, 2023, from https://ijpsr.com/bft-article/computer-based-screening-of-the-anticancer-property-of-selected-panax-ginseng-phyto-ligands DOI:10.13040/IJPSR.0975-8232.14(3).1714-27

Figures

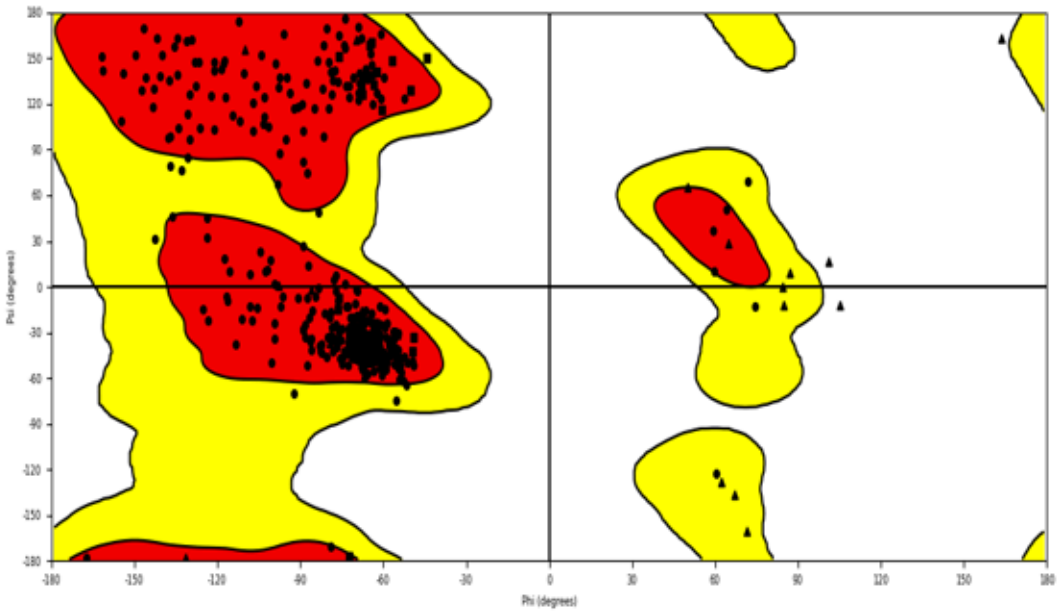

Figure 1

Ramachandran Plot of receptor T. cruzi 14-α-demethylase protease

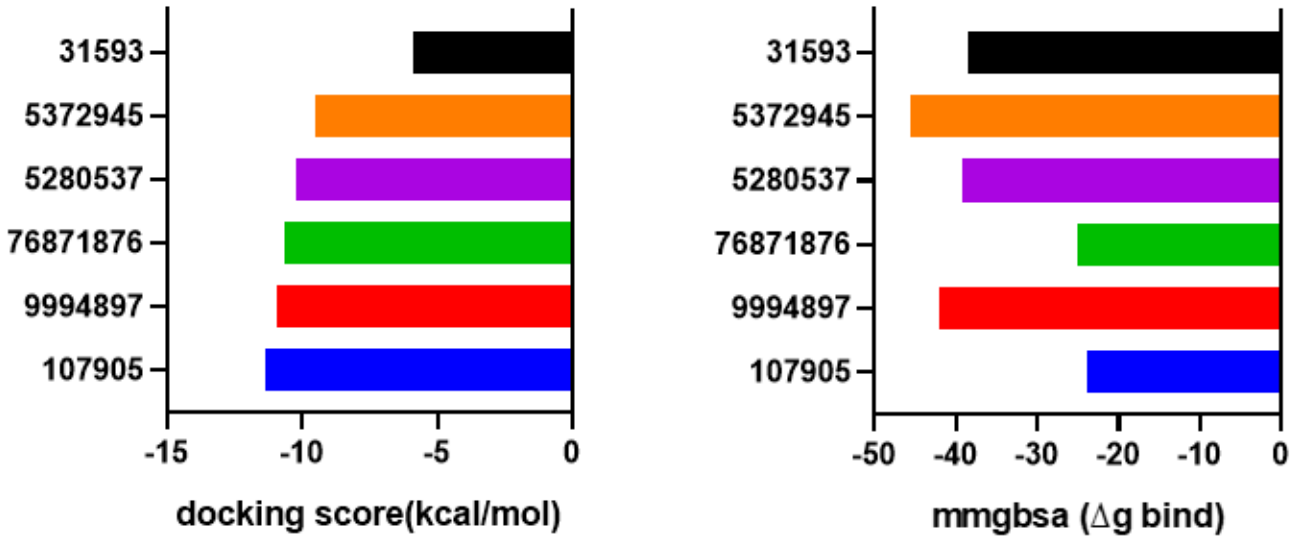

Figure 2

Graphical Representation Of The Binding Free Energy (Docking Score) And Prime/Mm-Gbsa (Δg bind) Binding Energy For Docking Complexes.

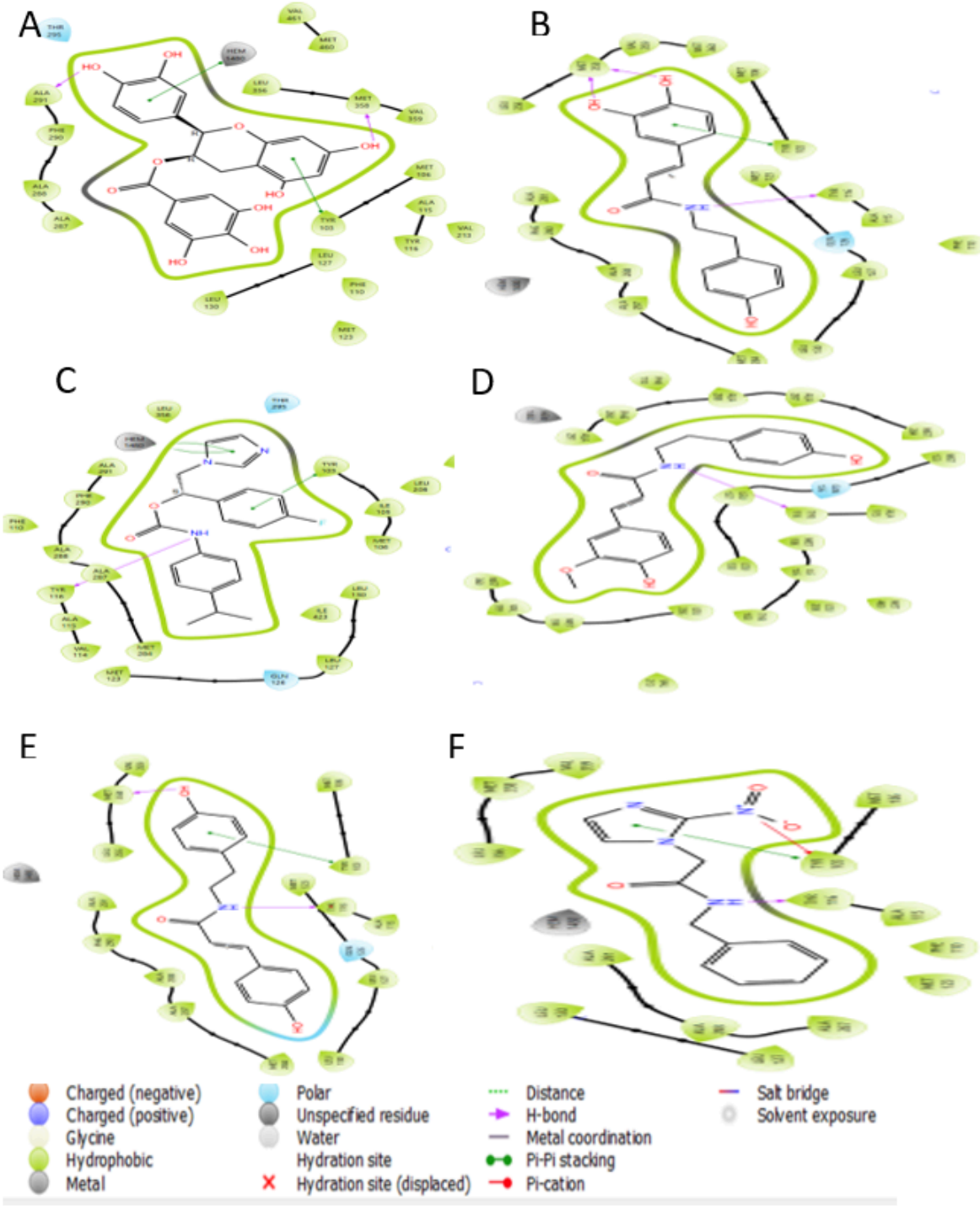

Figure 3

2D molecular interaction of hit compounds (*Tinospora Cordifolia*) with binding pocket of T. cruzi 14-α-demethylase protease(a) Epicatechin (b) N-trans-caffeoyltyramine (c) Co-crystallized Ligand (d) N-trans-Feruloyl tyramine (e) Paprazine (f) Benznidazole(standard)

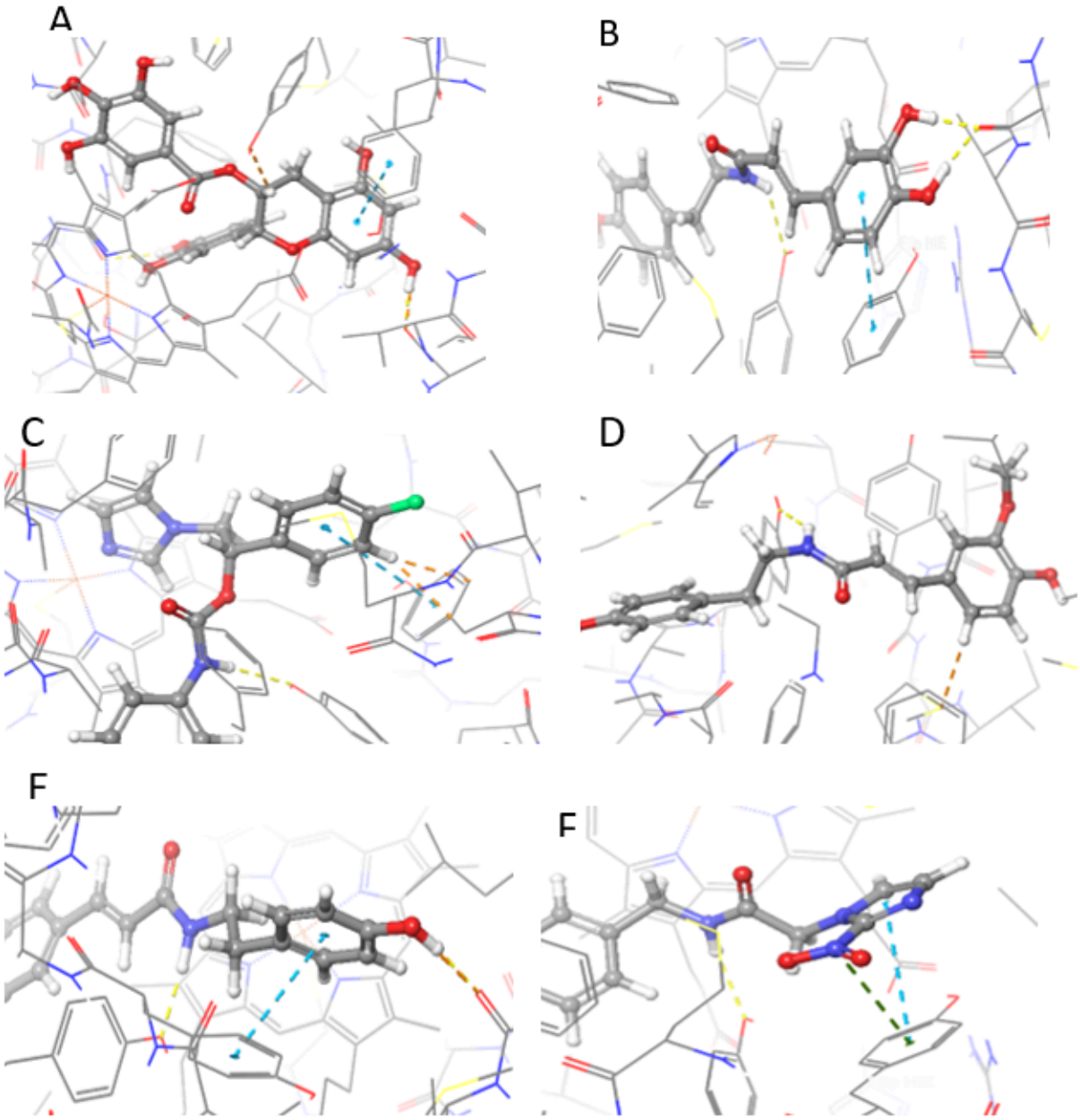

Figure 4

3D molecular interaction of hit compounds (*Tinospora Cordifolia*) with binding pocket of T. cruzi 14-α-demethylase protease(a) Epicatechin (b) N-trans-caffeoyl tyramine (c) Co-crystallized Ligand (d) N-trans-Feruloyl tyramine (e) Paprazine (f) Benznidazole(standard).

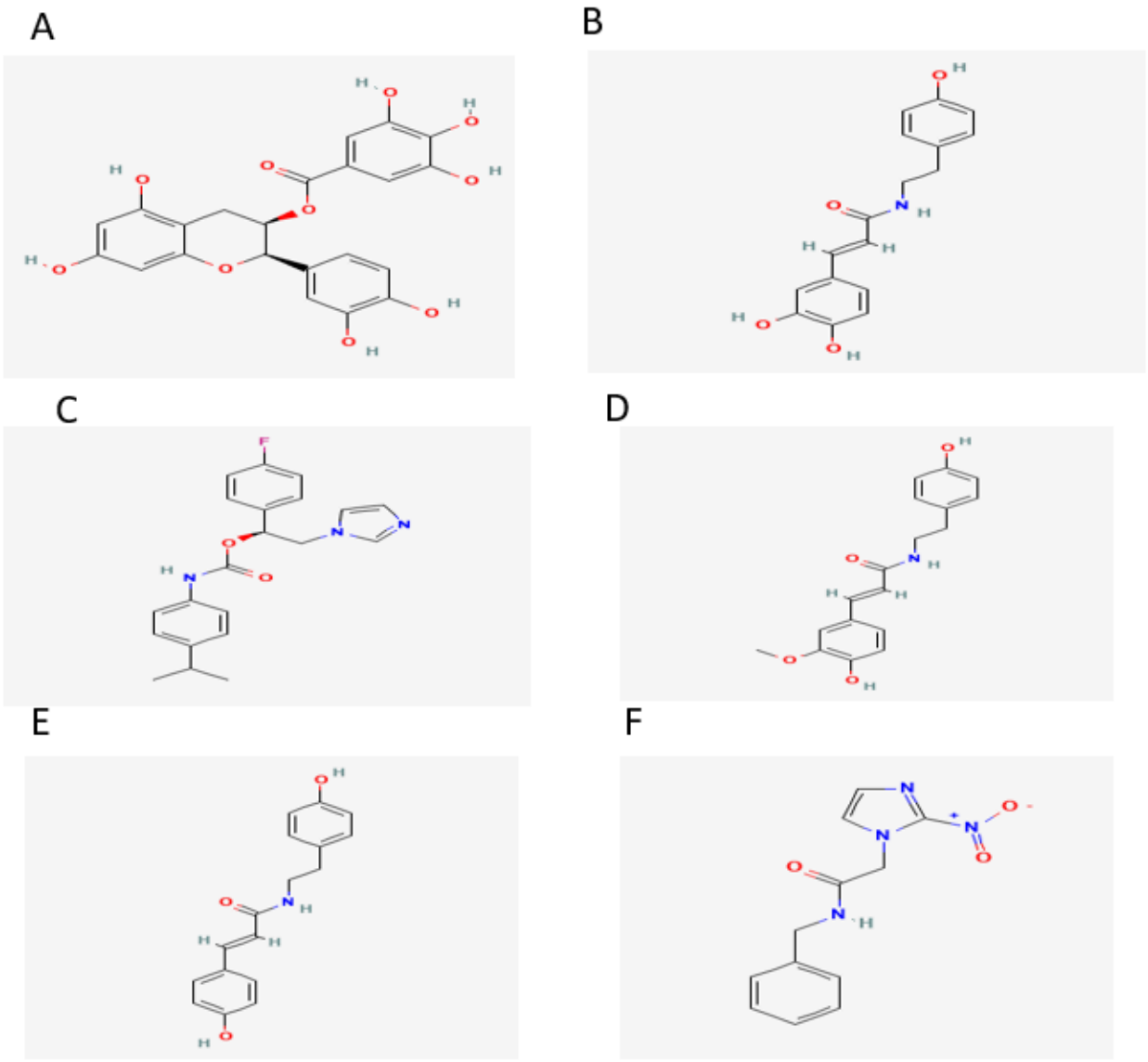

Figure 5

Chemical structure of hit compounds (*Tinospora Cordifolia*) (a) Epicatechin (b) N-trans-caffeoyltyramine (c) Co-crystallized Ligand (d) N-trans-Feruloyl tyramine (e) Paprazine (f) Benznidazole(standard).

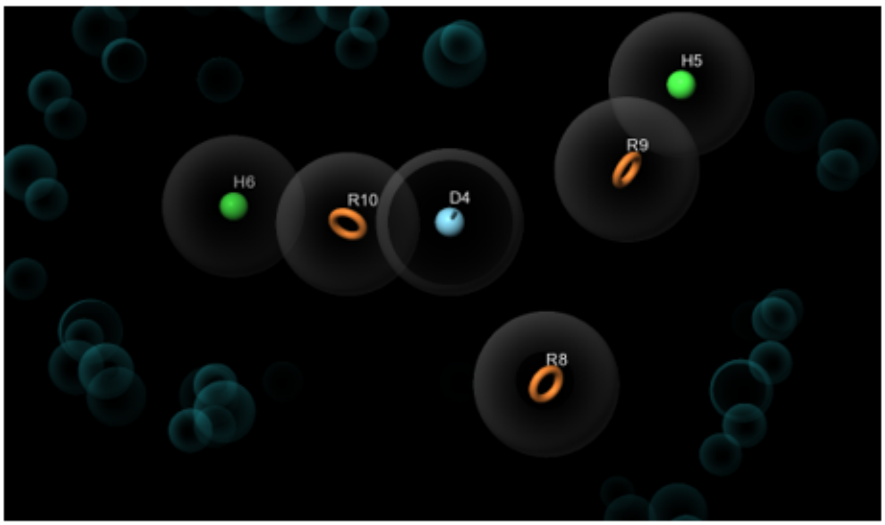

Figure 6

The H5 and H6 is Hydrophobic (green), R8,R10,R9 are Aromatic rings (orange) hydrogen bond donor (D4: blue) of the pharmacophore hypothesis.

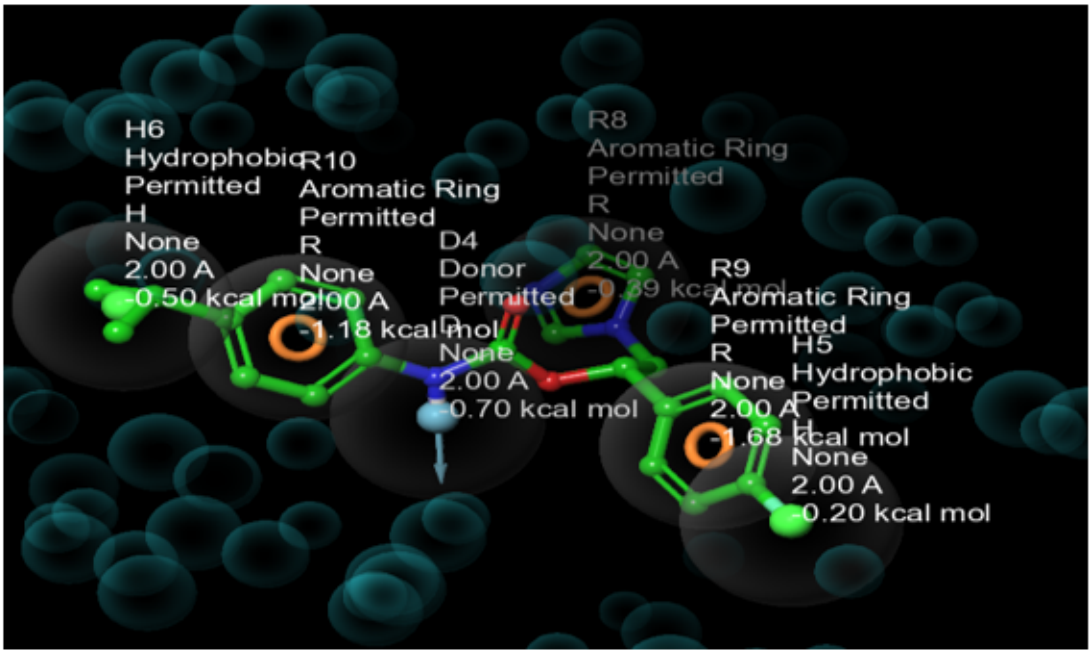

Figure 7

The pharmacophore hypothesis generated in complex with the reference ligand.

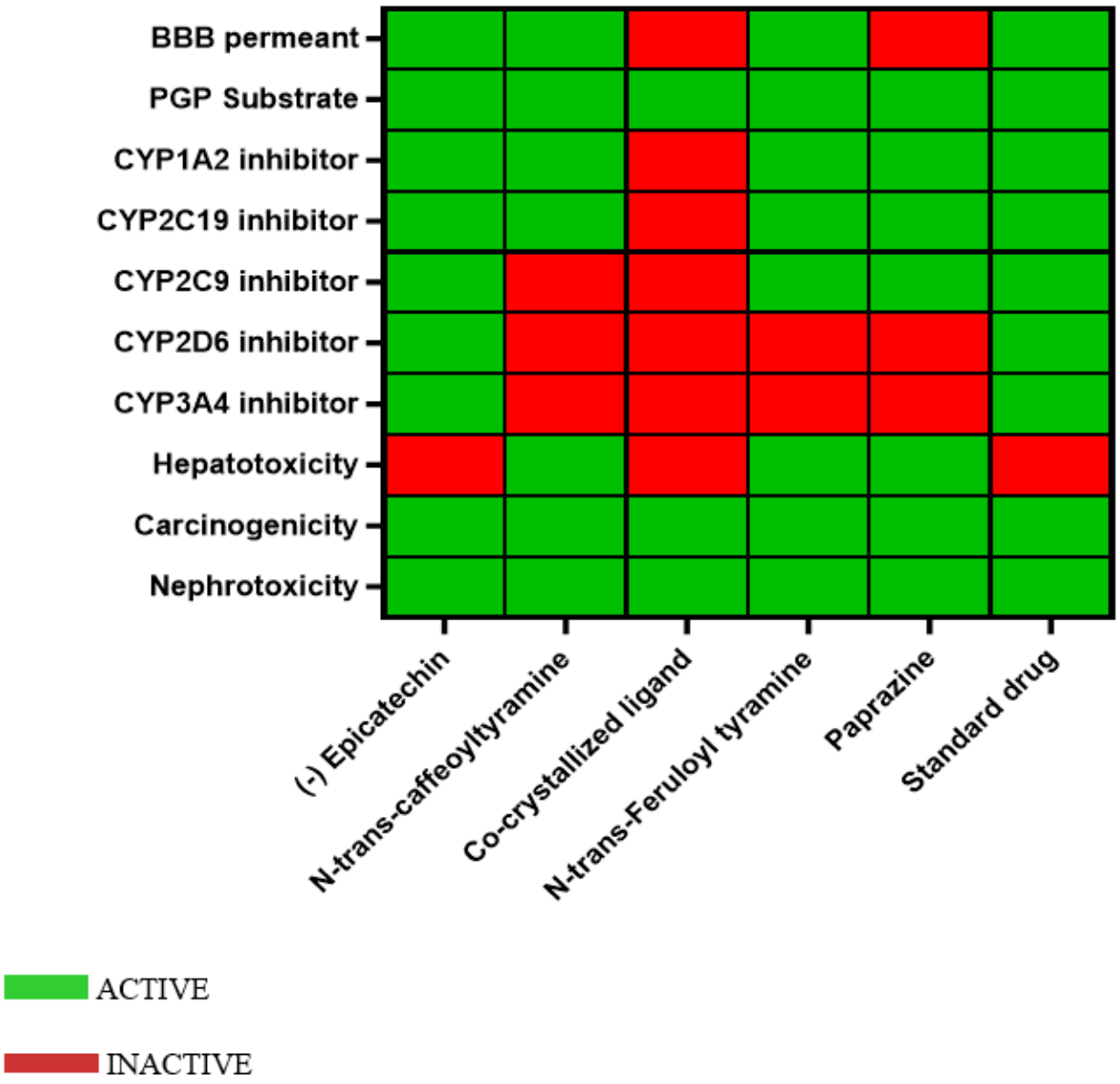

Figure 8

The Heat Map of The ADMET Parameter of Selected potentials of selected *Tinospora Cordifolia* phytochemical constituent, Co-crystallized ligand and standard drug.